

Non-equilibrium current via geometric scatterers

Pavel Exner

Doppler Institute for Mathematical Physics and Applied Mathematics,
Czech Technical University in Prague, Břehová 7, 11519 Prague,
and Nuclear Physics Institute ASCR, 25068 Řež near Prague, Czechia

E-mail: exner@ujf.cas.cz

Hagen Neidhardt

Weierstrass Institute, Mohrenstrasse 39, 10117 Berlin, Germany

E-mail: neidhard@wias-berlin.de

Miloš Tater

Nuclear Physics Institute ASCR, 25068 Řež near Prague, Czechia

E-mail: tater@ujf.cas.cz

Valentin A. Zagrebnov

Département de Mathématiques - Université d'Aix-Marseille (AMU)

163 av.de Luminy, 13288 Marseille Cedex 09, and

Institut de Mathématiques de Marseille (UMR 7373)

CMI-AMU, Technopôle Château-Gombert

39, rue F. Joliot Curie, 13453 Marseille Cedex 13, France

E-mail: valentin.zagrebnov@univ-amu.fr

Abstract. We investigate non-equilibrium particle transport in the system consisting of a geometric scatterer and two leads coupled to heat baths with different chemical potentials. We derive expression for the corresponding current the carriers of which are fermions and analyze numerically its dependence of the model parameters in examples, where the scatterer has a rectangular or triangular shape.

PACS numbers: 03.65.Nk, 72.20.Dp

Mathematics Subject Classification: 81Q35, 82B99

Keywords: non-equilibrium steady states, geometric scatterer

Dedicated to the memory of Markus Büttiker (1950-2013)

Contents

1	Introduction	2
2	Coupling of leads to the surface	4
3	Transport through the geometric scatterer	6
3.1	The transfer matrix	6
3.2	Transmission probability	7
3.3	The resonator quantities	9
4	Examples	10
4.1	A rectangular resonator	11
4.2	A triangular resonator	12
4.3	Stationary current	13

1. Introduction

The aim of the present paper is to analyze a stationary fermion transport, giving rise to electric current if the carrier particles are charged, between two heat baths connected through a geometric scatterer. By the latter we mean a quantum mechanical system of a mixed dimensionality consisting of a compact two-dimensional manifold G to which two (infinite) one-dimensional continuous leads are attached — cf. Fig. 1 — the latter are considered as heat and Fermi particle baths at equilibrium for given temperatures and chemical potentials. This assumption is made for simplicity. In general, one can think of the leads as of connecting links between the manifold and the baths, however, since in a one-mode quantum transport the particles are in the asymptotic regime once they leave the manifold, the identification of the leads with the baths is the easiest way.

The main tool for our analysis is the Landauer-Büttiker formula, which expresses a steady fermion current (in other words, a particle flux) through the sample (scatterer) in terms of the transmission probability for the scatterer and of the external reservoirs equilibrium states. Under quite general conditions the formula has been proved in [AJPP] for the quasi-free fermions transport in the framework of the C^* -scattering approach. In fact, this approach allows much more, namely to construct non-equilibrium steady states and to make contact with non-equilibrium statistical mechanics, see the three-volume review [AJP] for a thorough discussion.

We are not going to prove the Landauer-Büttiker formula in the present context, because for our restricted purpose of study only the fermion current it can be done repeating *verbatim* the argument used in the analogous situation in [CGZ10], where discrete leads and a discrete sample G were considered. The formula has two essential ingredients: *Fermi functions* for the thermal statistical distributions of non-interacting

fermions in the leads (reservoirs) and the quantum *transmission probability* between the leads, which results from the stationary scattering calculations of the single-particle passage throughout the sample.

In a sense the problem of a stationary current through the manifold G that we treat here can be regarded as a ‘continuous’ version of the model discussed in [CGZ10] describing a similar effect in the discrete setting. However, the continuous case has its peculiarities. While the difference is not very important for treating the leads, it becomes nontrivial in the analysis of scattering problem due to its mixed dimensionality, due to which the transport in such systems exhibits unusual and interesting features. Let us add that the way to describe quantum dynamics of such ‘strange’ scatterers can be traced back to [EŠ87]; it is based on construction of admissible Hamiltonians as self-adjoint extensions of a suitable symmetric operator, starting from the situation when different parts of the configuration space are decoupled.

Let us mention that the *ballistic* conductance — but not the current — for a mixed dimensionality scatterer was the subject of the paper [BGMP02] where the model of one-dimensional leads attached to a quantum sphere was investigated. From the quantum-mechanical point of view, the central problem both in [BGMP02] and in the present paper how to match wave-functions of the leads and the manifold G at the points of their junctions. The mentioned construction based on self-adjoint extension can be performed in different, equivalent ways, the result being always a family of boundary conditions involving appropriate generalized boundary values [EŠ87, BGMP02].

In the present paper we do not reduce ourselves to the linear response, i.e. to analysis of the conductance. We study the non-equilibrium current $I(V, V_g)$ throughout geometric scatterers as a function of two parameters: the difference: $V = \mu_2 - \mu_1 \geq 0$ of the two leads *electro-chemical* potentials with the aim to deduce the quantum *Ohm law*, and the *plunger gate* voltage V_g applied to the scatterer, which controls its *resonant* quantum conductance. Note that in contrast to [CGZ10] we consider here the two ‘external’ parameters *separately*. Of course, in certain cases it is plausible to work with the hypothesis $V = V_g$ which implies a highly non-linear current-voltage behaviour [CGZ10], however, the current-driving potential difference V and the gate voltage V_g controlling the conductance are *a priori* of a different nature. In particular, experimentally one can modify the quantum (resonant) conductance by varying V_g , see [CJM06].

What concerns the literature indicated above, the ballistic ($V_g = 0$) linear response $\sigma(\mu, 0) := \partial_V I(V, 0)|_{V=0}$ with $\mu = \mu_1 = \mu_2$, was the subject of [BGMP02], whereas the resonant conductance $\sigma(\mu, V_g)$ modification by variation of V_g was considered in [CJM06]. The present paper analyses the current-voltage dependence $I(V, V_g)$, that is, the Ohm law, parameterized by the plunger gate voltage V_g .

Let us briefly review the contents of the paper. In the next section we describe the construction used to couple the wave function and indicate which of the Hamiltonians obtained in this way might be physically the most relevant. Using the result, we solve in Sec. 3 the quantum-mechanical scattering problem finding the transmission probability

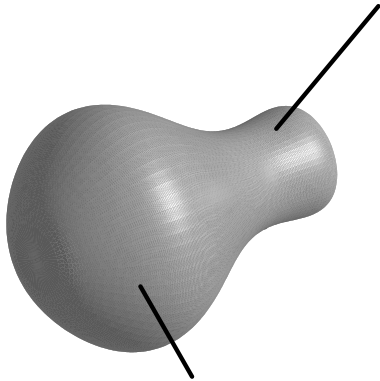


Figure 1. A geometric scatterer

as a function of the involved particle momenta; we shall also explain how the needed quantities can be computed for a compact manifold G . The concluding section is devoted to discussion of examples in which G is a two-dimensional rectangular and triangular ‘billiard’. Using the Landauer-Büttiker formula we compute the current and analyze numerically its dependence on the model parameters.

2. Coupling of leads to the surface

As we have said, the core of the model is the quantum-mechanical scattering on such a geometric object with leads attached. The first question to address is how they can be coupled mutually in a way which would conserve the probability current. Following [EŠ87] this question was investigated in various papers – one can mention, e.g., [EŠ97, Ki97, ETV01, BGMP02]. Their result cannot be directly used for our purpose, however, since in all those works it was assumed that the energy is conserved, i.e. that the particle momentum is the same on both the leads, and have to be modified. One can adopt the (quantum) transfer matrix approach,

$$\begin{pmatrix} u(0+) \\ u'(0+) \end{pmatrix} = L \begin{pmatrix} u(0-) \\ u'(0-) \end{pmatrix}. \quad (2.1)$$

with L derived in [ETV01] where $u(0\pm)$ and $u'(0\pm)$ are the boundary values of the wave functions on the leads at the junctions, however, using it as a component of our model, one has to take into account that the particles move with velocities given by the temperatures and chemical potentials of the reservoirs.

To construct the model indicated in the introduction one has to know how to describe motion of a quantum mechanical particle on a configuration space of a mixed dimensionality. A general prescriptions how the corresponding self-adjoint Hamiltonians can be constructed was first formulated in [EŠ87]. Since the most natural coupling is *local*, we may disregard geometrical peculiarities of the lead and the surface and illustrate the construction in the setting where a halfline is attached to a plane. The state Hilbert space is then $L^2(\mathbb{R}_-) \oplus L^2(\mathbb{R}^2)$ and if we neglect physical constants the Hamiltonian

acts on its elements as

$$\begin{pmatrix} \psi_{\text{lead}} \\ \psi_{\text{plane}} \end{pmatrix} \rightarrow \begin{pmatrix} -\psi_{\text{lead}}'' \\ -\Delta\psi_{\text{plane}} \end{pmatrix}.$$

To make such an operator self-adjoint one has to impose suitable boundary conditions which couple the wave-functions at the junction.

The boundary values to be used are obvious on the lead side being the columns $\psi_{\text{lead}}(0-)$ and $\psi'_{\text{lead}}(0-)$. On the other hand, in the plane we have to use generalized ones. To understand how to define them, we note that if we restrict two-dimensional Laplacian to functions vanishing at the origin and take the adjoint to such an operator, the functions in the corresponding definition domain will have a logarithmic singularity at the origin [EŠ87]. The said generalized boundary values $L_j(\psi_{\text{plane}})$, $j=0,1$, are then given as coefficients in the corresponding expansion,

$$\psi_{\text{plane}}(x) = L_0(\psi_{\text{plane}}) \ln|x| + L_1(\psi_{\text{plane}}) + o(|x|), \quad (2.2)$$

being defined as

$$L_0(\psi_{\text{plane}}) = \lim_{|x| \rightarrow 0} \frac{\psi_{\text{plane}}(x)}{\ln|x|}, \quad (2.3)$$

$$L_1(\psi_{\text{plane}}) = \lim_{|x| \rightarrow 0} \left[\psi_{\text{plane}}(x) - L_0(\psi_{\text{plane}}(|x|)) \ln|x| \right].$$

Using these notions we can write the sought boundary conditions as

$$\begin{aligned} \psi'_{\text{lead}}(0+) &= A\psi_{\text{lead}}(0+) + 2\pi\bar{C}L_0(\psi_{\text{plane}}), \\ L_1(\psi_{\text{plane}}) &= C\psi_{\text{lead}}(0+) + DL_0(\psi_{\text{plane}}), \end{aligned} \quad (2.4)$$

where $A, D \in \mathbb{R}$ and C is a complex number; it means, in particular, that the coupling depends on four real parameters. If C is chosen real we get a coupling invariant w.r.t. the time reversal which we will assume throughout in the following. It is worth noting that the above boundary conditions are generic but do not cover all the self-adjoint couplings leaving out cases when the coefficient matrix is singular; this flaw can be mended in the standard way [KS99] if one replaces (2.4) by the symmetrized form

$$\mathcal{A} \begin{pmatrix} \psi_{\text{lead}}(0+) \\ L_0(\psi_{\text{plane}}) \end{pmatrix} + \mathcal{B} \begin{pmatrix} \psi'_{\text{lead}}(0+) \\ L_1(\psi_{\text{plane}}) \end{pmatrix} = 0$$

with appropriately chosen matrices \mathcal{A}, \mathcal{B} . For our present purpose, however, the generic conditions (2.4) are sufficient.

The question which boundary conditions are physically ‘correct’ ones is difficult and the general answer to it is not known. We will not address it here and limit ourselves to mentioning that various choices are used:

- (i) the simplest possibility is to keep just the term coupling the two parts of the configuration manifold, i.e. to put $A = D = 0$.

- (ii) a heuristic way to choose the ‘natural’ coupling was suggested in [EŠ97]: comparing the scattering matrix of the coupling given by (2.4) with the low-energy behavior of scattering in the system of a plane to which a cylindrical ‘tube’ is attached, one arrives at the identification

$$A = \frac{1}{2\rho}, \quad B = \sqrt{\frac{2\pi}{\rho}}, \quad C = \frac{1}{\sqrt{2\pi\rho}}, \quad D = -\ln \rho, \quad (2.5)$$

where ρ is the contact radius; physical relevance of these conditions was illustrated in [EŠ97] by explaining the experimentally observed distribution of resonances in a microwave resonator with a thin antenna.

- (iii) the choice of the coupling amounts to fixing the singularity of the Hamiltonian Green’s function at the connection point. One can do that directly without using boundary conditions explicitly [Ki97].

What is important is the local character of the coupling which makes it possible to use the above description of the coupling in any situation where a one-dimensional segment is attached to a smooth two-dimensional surface; this is what we will use in the following.

3. Transport through the geometric scatterer

3.1. The transfer matrix

Equipped with the above notions we can now solve the quantum mechanical part of the problem. The first step consists of finding the transfer matrix (2.1) for our system. This part is essentially the same as in [ETV01] and we include it in order to make the paper self-contained. The compact manifold G describing the geometric scatterer may or may not have a boundary; we suppose that the two leads are attached to it at two different interior points x_1, x_2 of G . The manifold part of the Hamiltonian is the Laplace-Beltrami operator on the state Hilbert space $L^2(G)$ of the scatterer. It is coupled to the Laplacians on the two leads by the boundary conditions (2.4) with the coefficients indexed by $j = 1, 2$; later we will assume that the couplings are the same.

The most important object for us is the Green’s function $G(., .; k)$ of the Laplace-Beltrami operator, i.e. the integral kernel of its resolvent which exists whenever the k^2 does not belong to the spectrum. Its actual form depends on the geometry of G but the diagonal singularity does not. The reason is that the manifold G admits in the vicinity of any point a local Cartesian chart and the Green’s function behaves with respect to those variables as that of Laplacian in the plane,

$$G(x, y; k) = -\frac{1}{2\pi} \ln |x-y| + \mathcal{O}(1), \quad |x-y| \rightarrow 0. \quad (3.1)$$

Looking for transient solutions to the Schrödinger equation, we need a general solution to the Laplace-Beltrami equation on G for the energy k^2 . Without loss of generality, we may write it as

$$u(x) = a_1 G(x, x_1; k) + a_2 G(x, x_2; k), \quad (3.2)$$

where x_1, x_2 are the contact points [Ki97]. In view of (3.1) the singularities of u at x_1, x_2 have the character (2.2) and we can evaluate the generalized boundary values (labeled by the point at which they are taken) to be

$$L_0[x_j] = -\frac{a_j}{2\pi}, \quad L_1[x_j] = a_j \xi(x_j, k) + a_{3-j} G(x_1, x_2; k) \quad (3.3)$$

for $j = 1, 2$, where

$$\xi(x_j; k) := \lim_{x \rightarrow x_j} \left[G(x, x_j; k) + \frac{\ln |x - x_j|}{2\pi} \right]. \quad (3.4)$$

Let u_j be the wavefunction on the j -th lead. Using the abbreviations u_j, u'_j for its boundary values we infer from the boundary conditions (2.4) that

$$\begin{aligned} u'_1 &= A_1 u_1 - 2\pi \bar{C}_1 a_1, & a_1 \xi_1 + a_2 g &= C_1 u_1 - \frac{D_1 a_1}{2\pi}, \\ u'_2 &= -A_2 u_2 + 2\pi \bar{C}_2 a_2, & a_2 \xi_2 + a_1 g &= C_2 u_2 - \frac{D_2 a_2}{2\pi}, \end{aligned}$$

where we have denoted $g := G(x_1, x_2; k)$. Note that in the first equation of the second pair we used the opposite sign, because it is natural to identify the second (i.e., the ‘right’) lead with \mathbb{R}_+ . It is straightforward to rewrite these equations as a linear system with the unknown u_2, u'_2, a_1, a_2 and to solve it; this gives in particular the transfer matrix,

$$L = \frac{1}{g C_2} \begin{pmatrix} C_1 Z_2 + \frac{A_1 \mathcal{D}}{C_1} & -\frac{\mathcal{D}}{C_1} \\ |C_2|^2 \left(C_1 - Z_1 \frac{A_1}{C_1} \right) - C_1 A_2 Z_2 - \frac{A_1 A_2}{C_1} \mathcal{D} & \frac{A_2 \mathcal{D}}{C_1} + \frac{|C_2|^2 Z_1}{C_1} \end{pmatrix}, \quad (3.5)$$

where $Z_j := \frac{D_j}{2\pi} + \xi_j$ and $\mathcal{D} := g^2 - Z_1 Z_2$; in these formula $\xi_j := \xi(x_j; k)$. It is easy to check that

$$\det L = -\frac{\bar{C}_2 C_1}{\bar{C}_1 C_2}, \quad (3.6)$$

hence $\det L = -1$ as long as we suppose that the coupling is time-reversal invariant and the parameters C_j are real. Note that the same is true even without this assumption if the couplings are the same. We adopt in the following both hypotheses so that our model will be characterized by three real parameters A, C, D ; in that case the transfer matrix (3.5) simplifies to the form

$$L = \frac{1}{g} \begin{pmatrix} Z_2 + \frac{A}{C^2} \mathcal{D} & -2\frac{\mathcal{D}}{C^2} \\ C^2 - A(Z_1 + Z_2) - \frac{A^2}{C^2} \mathcal{D} & \frac{A}{C^2} \mathcal{D} + Z_1 \end{pmatrix}. \quad (3.7)$$

3.2. Transmission probability

To make use of the Landauer-Büttiker formula we have to know the S -matrix, in particular the transmission amplitude via a quantum gate (dot) for the process in question. To fix direction of the particle current note that according this formula

electrons (fermions \ddagger) are moving from the ‘left’ ($x < 0$ and μ_2) to the ‘right’ ($x > 0$ and μ_1) lead *if* the bias of *electro-chemical* potentials in these leads is *positive*, i.e. $V = \mu_2 - \mu_1 > 0$.

On the other hand in the nonballistic regime, $V_g \neq 0$, the incoming (‘left’) and outgoing (‘right’) particles may have different momenta k_1, k_2 , hence the formula relating L and S derived in [ETV01] is not applicable. It is not difficult, however, to derive a more general result to replace it. To this aim, we write the scattering solutions to the ‘left’ and ‘right’ of the manifold G as

$$\begin{aligned} u_1(x) &= e^{ik_1x} + r e^{-ik_1x} \quad \dots \quad x < 0 \\ u_2(x) &= t e^{ik_2x} \quad \dots \quad x > 0 \end{aligned} \tag{3.8}$$

From this Ansatz we get the boundary values $u_1^{(\iota)}(0-)$ and $u_2^{(\iota)}(0-)$, $\iota = 0, 1$, which will enter the coupling conditions (2.4) as $\psi_{\text{lead}}(0)$ and $\psi'_{\text{lead}}(0)$ for the ‘left’ and ‘right’ lead, respectively. The relation between k_1 and k_2 is determined by the conservation of energy, i.e. by the fact that their squares differ by V_g . On the other hand, there is no *a priori* rule relating the energy k^2 describing the particle in the resonator to k_j^2 , $j = 1, 2$. We adopt the most simple choice as a *model assumption* setting

$$k_j = \sqrt{k^2 - \frac{1}{2}(-1)^j V_g}, \quad j = 1, 2, \quad , \tag{3.9}$$

note that such a fixing of the energy scale of the scatterer with respect to those of the leads can be equivalently regarded as a choice of the ‘plunger gate voltage’ V_g [CJM06]. For the sake of definiteness we suppose that $V_g > 0$.

For the moment, however, we keep the three values independent. Inserting the boundary values obtained from (3.8) into (2.1) we get the relations

$$\begin{aligned} t &= L_{11} + ik_1 L_{12} + r(L_{11} - ik_1 L_{12}) \\ ik_2 t &= L_{21} + ik_1 L_{22} + r(L_{21} - ik_1 L_{22}) \end{aligned}$$

which represent a system of equations for the reflection and transmission amplitudes being easily solved by

$$\begin{aligned} r &= - \frac{L_{21} + i(k_1 L_{22} - k_2 L_{11}) + k_1 k_2 L_{12}}{L_{21} - i(k_1 L_{22} + k_2 L_{11}) - k_1 k_2 L_{12}}, \\ t &= - \frac{2ik_1}{L_{21} - i(k_1 L_{22} + k_2 L_{11}) - k_1 k_2 L_{12}}. \end{aligned} \tag{3.10}$$

In particular, substituting the elements of the transfer matrix (3.7) into these solutions, we obtain the transmission probability $t(k_1, k_2, k)$ of our model in the form

$$- \frac{2ik_1 g}{C^2 - A(Z_1 + Z_2) - \frac{A^2}{C^2} \mathcal{D} - ik_1 \left(\frac{A}{C^2} \mathcal{D} + Z_1 \right) - ik_2 \left(Z_2 + \frac{A}{C^2} \mathcal{D} \right) + 2k_1 k_2 \frac{\mathcal{D}}{C^2}}, \tag{3.11}$$

\ddagger For definiteness, we think of an electric current between the reservoirs connected through a heterostructure modeled by the manifold G , however, the results apply to transport of arbitrary fermions.

the quantities g , Z_j , \mathcal{D} being functions of k . Needless to say, we consider only the situation when the leads are not decoupled from the resonator, $C \neq 0$, in which case the expression in the denominator makes sense.

The behaviour of the function t is in general quite complex. It has been analyzed in previously in a particular situation when $k_1 = k_2 = k$ (i.e., in the ballistic regime, $V_g = 0$) and G is a sphere to which the leads are coupled in polar or non-polar positions and in particular ways [Ki97, ETV01, BGMP02]. Such systems have numerous resonances corresponding to energies for which the terms linear in the momentum dominate in the denominator, while away from them the transmission is governed by the quadratic term and decreases with increasing energy. It is expected that the same will be true for a much wider class of geometric scatterers.

3.3. The resonator quantities

To make use of the above results one must be able to evaluate the functions g , Z_j , \mathcal{D} entering the formula (3.11). Since G is supposed to be compact, so the Laplace-Beltrami operator on it has a purely discrete spectrum, one can use the corresponding spectral analysis; we recall the procedure following again essentially the discussion in [ETV01]. The eigenvalues $\{\lambda_n\}_{n=1}^\infty$ number in the ascending order with the multiplicity taken into account correspond to eigenfunctions $\{\phi_n\}_{n=1}^\infty$ which form an orthonormal basis in $L^2(G)$. The common Green's function expression then gives

$$g(k) = \sum_{n=1}^{\infty} \frac{\phi_n(x_1)\overline{\phi_n(x_2)}}{\lambda_n - k^2}. \quad (3.12)$$

To express the remaining three values. Z_1 , Z_1 and \mathcal{D} , we have to compute the regularized limit (3.4). Expanding the logarithm into the Taylor series, we can rewrite the sublimit expression as

$$G(x_j + \sqrt{\varepsilon}n, x_j; k) + \frac{\ln \sqrt{\varepsilon}}{2\pi} = \sum_{n=1}^{\infty} \left(\frac{\phi_n(x_j + \sqrt{\varepsilon}n)\phi_n(x_j)}{\lambda_n - k^2} - \frac{(1-\varepsilon)^n}{4\pi n} \right),$$

where n is a unit vector in the local chart around the point x_j . Unfortunately, interchanging the limit with the sum is not without risk since the series does not converge uniformly; to see that the result may indeed depend on the regularization procedure, it is sufficient to replace $\sqrt{\varepsilon}$ by $c\sqrt{\varepsilon}$ at the left-hand side. To gauge the possible non-uniqueness, let us compute the difference

$$\xi(x_j, k) - \xi(x_j, k') = \lim_{\varepsilon \rightarrow 0^+} \sum_{n=1}^{\infty} \left(\frac{\phi_n(x_j + \sqrt{\varepsilon}n)\overline{\phi_n(x_j)}}{\lambda_n - k^2} - \frac{\phi_n(x_j + \sqrt{\varepsilon}n)\overline{\phi_n(x_j)}}{\lambda_n - k'^2} \right).$$

This sum is already uniformly convergent, because by standard semiclassical estimates [RS78, XIII.16] the sequence $\{\|\phi_n\|_\infty\}_{n=1}^\infty$ is bounded under our assumptions and $\lambda_n = 4\pi|G|^{-1}n + \mathcal{O}(1)$ as $n \rightarrow \infty$, hence

$$\frac{1}{\lambda_n - k^2} - \frac{1}{\lambda_n - k'^2} \sim \frac{1}{n^2},$$

and therefore

$$\xi(x_j, k) - \xi(x_j, k') = \sum_{n=1}^{\infty} \left(\frac{|\phi_n(x_j)|^2}{\lambda_n - k^2} - \frac{|\phi_n(x_j)|^2}{\lambda_n - k'^2} \right). \quad (3.13)$$

From the same reason one can claim that

$$\tilde{\xi}(x_j, k) := \sum_{n=1}^{\infty} \left(\frac{|\phi_n(x_j)|^2}{\lambda_n - k^2} - \frac{1}{4\pi n} \right) \quad (3.14)$$

makes sense and $\xi(x_j, k) - \tilde{\xi}(x_j, k)$ is independent of k . We have therefore

$$\xi(x_j, k) = \sum_{n=1}^{\infty} \left(\frac{|\phi_n(x_j)|^2}{\lambda_n - k^2} - \frac{1}{4\pi n} \right) + c(G). \quad (3.15)$$

The constant $c(G)$ depends on the manifold G only and we may neglect it unless a particular coupling has to be fixed, because a nonzero value of $c(G)$ amounts just to a coupling renormalization: D_j has to be changed to $D_j + 2\pi c(G)$. Little is known about a proper choice of $c(G)$, we can only recall that for a flat rectangular G treated in [EŠ97] an agreement with the experiment was found using $c(G) = 0$.

Remark: Note that there is another way to switch on the plunger gate potential directly on the resonator, see [CJM06]. It is experimentally realizable as a shift of the resonator spectrum by the gate voltage \widehat{V}_g : $\{\lambda_n \rightarrow \widehat{\lambda}_n\}_{n=1}^{\infty}$, where $\widehat{\lambda}_n := \lambda_n + \widehat{V}_g$. To include this kind of the gate potential into our scheme we have only to modify correspondingly the Green function $G \rightarrow \widehat{G}$ by the spectral shift \widehat{V}_g and to recalculate the coefficients in representation (3.11).

4. Examples

We stress that the voltage difference appearing in (3.9) in itself does not produce any particle current although the S -matrix is in general nontrivial. It is the lack of equilibrium between fermions in the two leads (playing role of external heat baths). It is true even in the ballistic regime when we consider an infinitesimal difference between the two equilibria. As mentioned in the introduction, the non-equilibrium stationary flux of particles is expressed by the Landauer-Büttiker formula, which involves the quantum mechanical transmission probability and two non-equal Fermi-Dirac functions for the left and right lead — see, e.g., [CGZ10].

Our main aim now is to find the conductivity of the geometric scatterer for different values of the electro-chemical potentials μ_1, μ_2 and/or different temperatures. The quantity of interest is the stationary current I between the two leads,

$$I = 2\pi \int_{V_g/2}^{\infty} [f_{\beta}(\lambda - \mu_2) - f_{\beta}(\lambda - \mu_1)] |t(k_1, k_2, k)|^2 d\lambda, \quad (4.1)$$

where λ is related to the sample energy by $k = \sqrt{\lambda}$ and the momenta k_j are given by (3.9), and furthermore, f is the Fermi-Dirac function,

$$f_{\beta}(\lambda) := \frac{1}{e^{\beta\lambda} + 1} \quad (4.2)$$

corresponding to the temperature β^{-1} . The conductivity σ is obtained as derivative of I with respect to the corresponding potential bias $V = \mu_2 - \mu_1 > 0$. In particular, if the potential difference is infinitesimal (the so-called *linear-response regime*), we obtain for the conductivity the usual Landauer-Büttiker formula in which $|t(k_1, k_2, k)|^2$ is integrated over $-\partial_\lambda f(\lambda - \mu)$, where $\mu = \mu_1 = \mu_2$ as, for instance, in [BGMP02] for the ballistic regime $k = k_1 = k_2$. Since spherical scatterers were analyzed in this paper as well as in [ETV01], we shall treat in the following two other examples.

4.1. A rectangular resonator

In the first one G is a rectangle with Dirichlet boundary. We note first that numerical treatment of (3.11) requires certain caution, cf. the discussion in [CJM06] for the discrete case. All the three quantities g , Z_j , \mathcal{D} entering the formula (3.11) are infinite series depending on k whose terms are indexed by a pair of indices (the formal index n is a pair $n = (n_x, n_y)$). It is useful to limit the maximal eigenvalue λ_{\max} first, then find all levels below this value and sum over all the corresponding pairs of indices.

We use the standard eigenfunctions and eigenvalues [EŠ97] to compute (3.12) and (4.1) (putting $c(G) = 0$ following [EŠ97] as mentioned above), to be inserted into (3.11). If the rectangle is $[0, c_1] \times [0, c_2]$, then

$$\psi_{n_x, n_y}(x, y) = \frac{2}{\sqrt{c_1 c_2}} \sin\left(n_x \frac{\pi}{c_1} x\right) \sin\left(n_y \frac{\pi}{c_2} y\right)$$

and

$$\lambda_{n_x, n_y} = \left(\frac{n_x \pi}{c_1}\right)^2 + \left(\frac{n_y \pi}{c_2}\right)^2$$

are the eigenfunctions and eigenvalues, respectively.

The series converge slowly. In order to achieve three-digit precision we had to sum up typically $5 \cdot 10^6$ terms. We present our results on Figs. 2 and 3.

We chose $c_1 = 2$, $c_2 = 1$ and three positions where the leads are attached as follows: the incoming one is always attached at $x_1 = 0.2$, $y_1 = 0.1$ and the three outgoing positions are $x_2 = 1.8$, $y_2 = 0.9$, or $x_2 = 0.2$, $y_2 = 0.9$, or $x_2 = 1$, $y_2 = 0.5$, respectively. Fig. 2 shows dependence of transmission probability $|t|^2$ on the energy λ of the particle in the resonator for the three indicated positions of outgoing leads. We see that some resonances appear at the same energy values, however, their significance changes being influenced, in particular, by the value of the eigenfunctions, which generates them, at the junction point.

Note that the transmission probability coefficient $|t|^2$ may in general exceed unity. It is clear from (3.8) and (3.9) that the necessary condition for this to happen is $V_g > 0$ because the scattering unitarity requires, in particular, that $|r|^2 + \left(\frac{k_2}{k_1}\right)^2 |t|^2 = 1$. Knowing the transmission probability we can proceed to compute the current. As this part does not differ substantially for different shapes of the scatterer, we will work it out only in the situation of our following example.

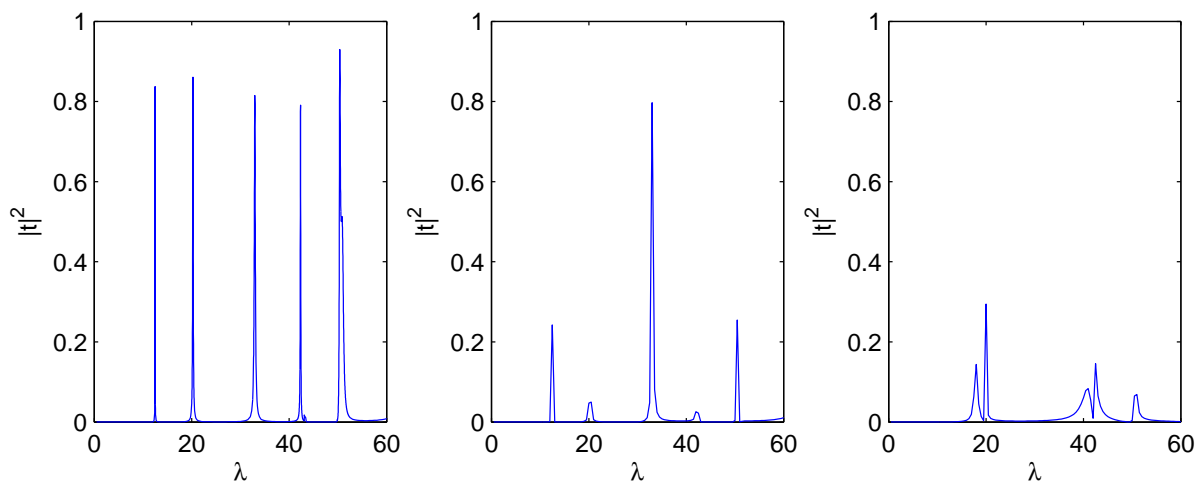


Figure 2. Dependence of $|t|^2$ on $\lambda = k^2$ for three positions of outgoing leads, namely $x_2 = 1.8, y_2 = 0.9$, or $x_2 = 0.2, y_2 = 0.9$, or $x_2 = 1, y_2 = 0.5$, respectively. The incoming lead is always attached at $x_1 = 0.2, y_1 = 0.1$.

4.2. A triangular resonator

In our next example G has a triangular shape. There are three triangular figures with Dirichlet boundary conditions for which the Laplacian eigenfrequencies and eigenfunctions are expressible via elementary transcendental functions [Ju80]. We choose the triangle with vertices $v_x^{(1)} = 0, v_y^{(1)} = 0, v_x^{(2)} = 0, v_y^{(2)} = 4\sqrt{3}, v_x^{(3)} = 3, v_y^{(3)} = \sqrt{3}$. The eigenfrequencies are labeled by two positive integers k, n with $n > k$, either both even or both odd,

$$\lambda_{n,k} = \frac{\pi^2}{108}(k^2 + 3n^2).$$

All the eigenfrequencies are simple. The corresponding eigenfunctions (normalized to unity) read

$$\begin{aligned} \psi_{k,n}(x, y) = & \frac{\sqrt{2}}{3\sqrt[4]{3}} \left(\sin\left(\frac{\pi nx}{6}\right) \sin\left(\frac{\pi k(y+2\sqrt{3})}{6\sqrt{3}}\right) + \right. \\ & \sin\left(\frac{\pi n(\sqrt{3}x-3y)}{12\sqrt{3}}\right) \sin\left(\frac{\pi k(\sqrt{3}x+y-4\sqrt{3})}{12\sqrt{3}}\right) - \\ & \left. \cos\left(\frac{\pi(\sqrt{3}nx+3ny-6\sqrt{3})}{12\sqrt{3}}\right) \sin\left(\frac{\pi k(\sqrt{3}x-y+4\sqrt{3})}{12\sqrt{3}}\right) \right). \end{aligned} \quad (4.3)$$

Next we have to choose points where to attach the leads. There are some interesting combinations, in particular,

- (i) near the vertex $v^{(1)}$, $x_1 = 0.1, y_1 = 0.2$, and in the center of mass, $x_2 = 1, y_2 = 5/\sqrt{3}$
- (ii) from the maximum of the ground state $x_1 = 1.195408, y_1 = 2.392313$ to the maximum of the first excited state $x_2 = 1.142144, y_2 = 1.645060$, i.e. between

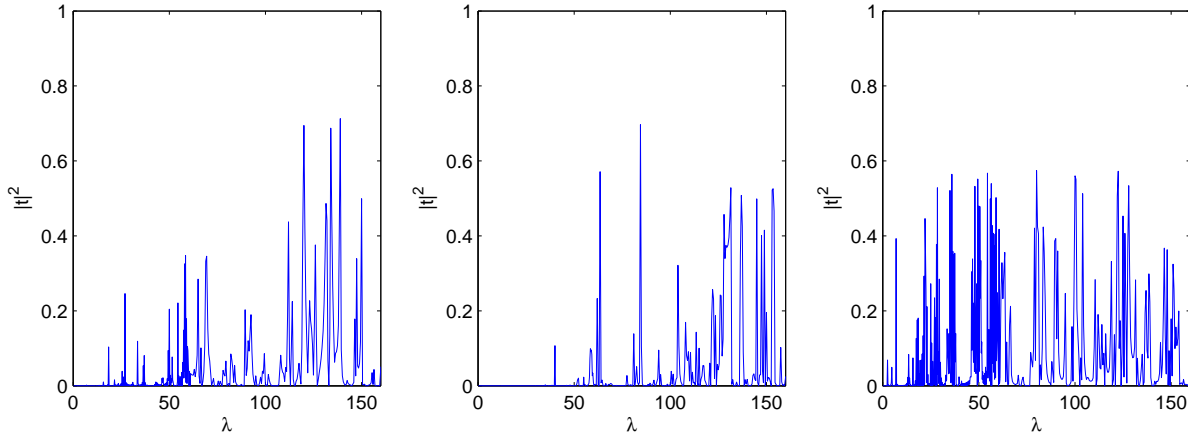


Figure 3. Dependence of $|t|^2$ on λ and on the points, where the leads are attached. The positions are described in the text below formula (4.3).

two points in central area

- (iii) between two most distant vertices $v^{(1)}$ and $v^{(2)}$, $x_1 = 0.1$, $y_1 = 0.2$ and $x_2 = 0.1$, $y_2 = 6.6$.

4.3. Stationary current

Let us now compute the stationary current $I = I(\mu_1, \mu_2, V_g)$ for the triangular resonator and inspect its dependence on the parameters of the model. It is clear from (4.1) it can be quite intricate and several factors play role, in particular, the spectral properties of the resonator together with the plunger-gate voltage V_g and junction positions, all those determining the transmission probability $|t(k_1, k_2, k)|^2$, in combination with the smearing coming from the shifted Fermi-Dirac functions $f_\beta(\lambda - \mu_2) - f_\beta(\lambda - \mu_1)$. It is clear that the latter approaches the characteristic function of the interval (μ_1, μ_2) in the zero-temperature limit, $\beta \rightarrow \infty$.

For the sake of definiteness we always consider the situation (i) considered above, i.e. one lead attached near the vertex $v^{(1)}$, $x_1 = 0.1$, $y_1 = 0.2$, and the other in the center of mass, $x_2 = 1$, $y_2 = 5/\sqrt{3}$. We start with the ballistic regime, $V_g = 0$. In the next Figure 4 we plot the current $I = I(\mu_1, \mu_2, 0)$ as a function of the potential bias $V = \mu_2 - \mu_1$ for four different choices of μ_1 and the inverse temperature $\beta = 25$. We see that $I(\mu_1, \mu_1 + V, 0)$ as a function of V is monotonous increasing. This fact can be easily understood looking at the shape of the function $f_\beta(\lambda - \mu_1 - V) - f_\beta(\lambda - \mu_1)$ which smears the spectral peaks of $|t(k_1, k_2, k)|^2$; at the considered high low temperature it is roughly a box the width of which increases with V ; the curve keeps roughly its shape and moves to the left as μ_1 increases.

Considering the ballistic regime again, we illustrate in Figure 5 variation of the current $I(\mu_1, \mu_2 = \mu_1 + V, 0)$ as a function of the electrochemical potential μ_1 in the left reservoir for several values of the potential bias $V = \mu_2 - \mu_1$. The plot

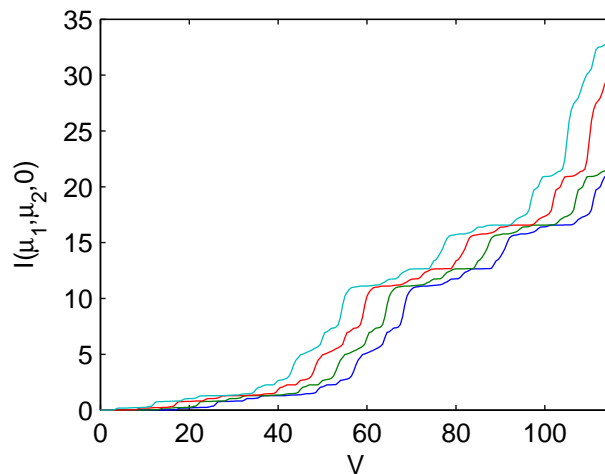


Figure 4. Variation of the current I_∞ in the ballistic regime, $V_g = 0$, as a function of the bias $V = \mu_2 - \mu_1$. Four choices are shown, $\mu_1 = 1, 5, 10, 15$, with $\beta = 25$, and the plot moves to the *left* as μ_1 increases; in the colour-online version they are represented by curves in blue, green, red, and cyan, respectively.

is again easily understood taking into account the almost-box-shape of the function $f_\beta(\lambda - \mu_1 - V) - f_\beta(\lambda - \mu_1)$: its width increases with V , and as a consequence the resonance peak structure becomes washed out for large bias. Another effect to notice concerns the behaviour for small μ_1 . If the bias is small, the current is negligible there, since the transmission probability $|t(k_1, k_2, k)|^2$ is tiny only for the spectral parameter $\lambda \lesssim 15$; it becomes visible at larger values of V due to the ‘Fermi-Dirac averaging’.

Still in the ballistic regime, Figure 6 treats the same situation as before, now illustrating the dependence of the current on the temperature. We choose a small potential bias, $V = 2$. In the low-temperature regime the transmission probability $|t(k_1, k_2, k)|^2$ is then integrated with a function close to a narrow box which produces a plot ‘interpolating’ between the first two graphs of Figure 4.3. If the temperature is considerably higher, $f_\beta(\lambda - \mu_1 - V) - f_\beta(\lambda - \mu_1)$ turns into a widely spread smooth peak leading again to washing out the resonance structure.

Turning to the non-ballistic regime, we illustrate in the next figures the dependence of the current $I(\mu_1, \mu_2 = \mu_1 + V, V_g)$ on the plunger-gate potential V_g , according to our convention considered nonnegative. We choose again a small potential bias, $V = 1$, and four different values of the electrochemical potential μ_1 . For zero temperature the only contribution to the current comes in view of (4.1) from the values of the spectral parameter λ belonging to the interval (μ_1, μ_2) , and it follows from assumption (3.9) that the current vanishes unless $V_g \leq 2\mu_2$. This no longer true for positive temperatures, however, in the low temperature regime such as $\beta = 25$ considered in Figure 7 the current above the value $2\mu_2$ is still negligible. This is easy to understand taking into account the exponential fall-off of the smearing function. Figure 7 also shows that below this threshold value the current increases. This effect comes from the increase of the transmission probability $|t(k_1, k_2, k)|^2$ with the of the plunger-gate potential V_g . We

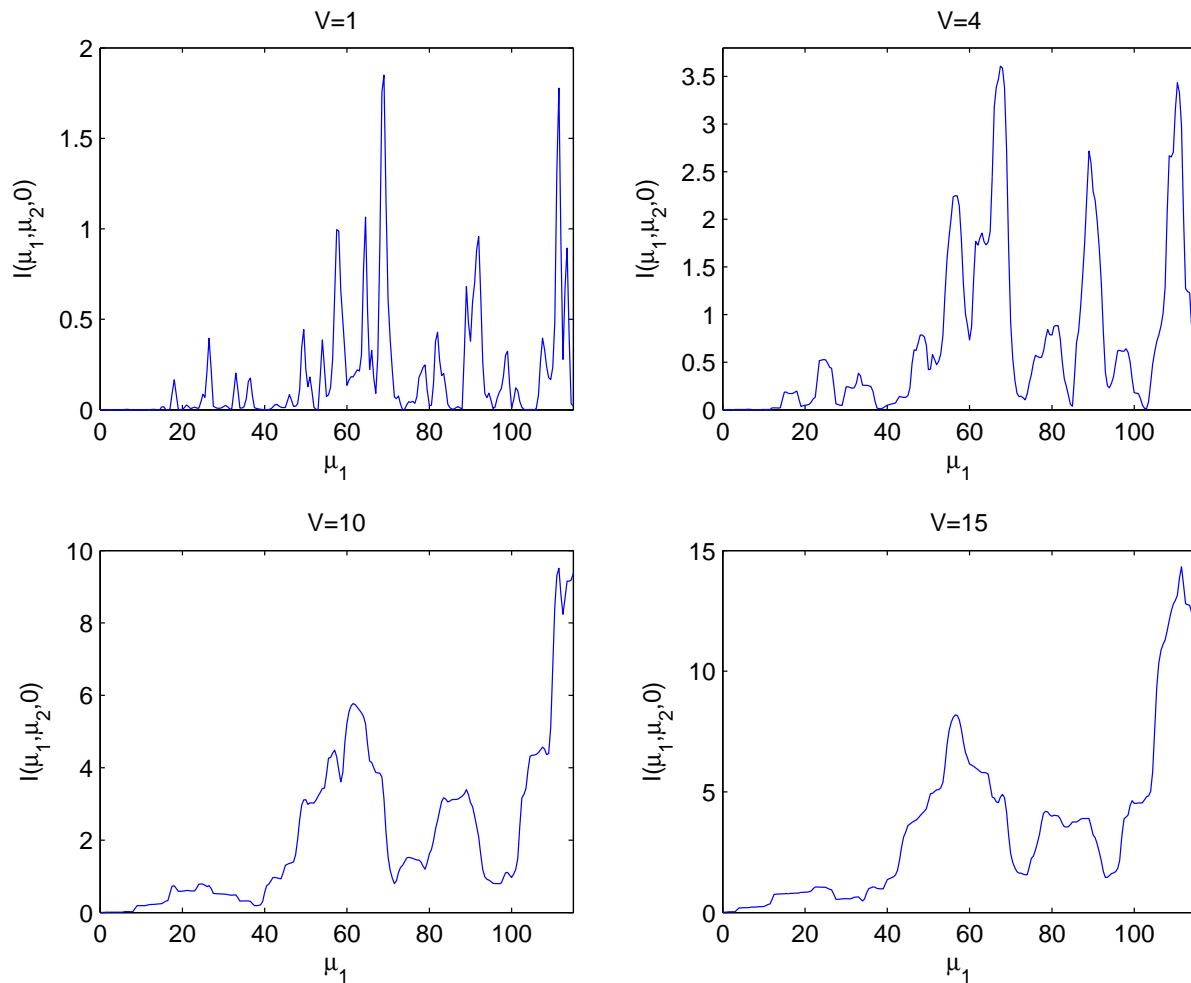


Figure 5. Variation of the current I_∞ in the ballistic regime, $V_g = 0$, as a function of μ_1 , while the potential bias $V = \mu_2 - \mu_1$ is fixed; we present four choices of $V = 1, 4, 10, 15$, with $\beta = 25$.

have remarked at the end of Sec. 4.1 that this quantity may exceed one for $V_g > 0$, and without showing the graph we claim that it indeed happens here for V_g large enough.

However, the increase is in general not monotonous, because the resonance effects are not complete suppressed by the smearing with $f_\beta(\lambda - \mu_1 - V) - f_\beta(\lambda - \mu_1)$. This is shown on our last picture, Figure 8, where we plot again the current *vs.* the plunger-gate voltage. Now we stay below the ‘threshold’ value $2\mu_2$ and we see that the plot may have peaks depending on both values of the electrochemical potentials. Furthermore, we illustrate how the plot changes with μ_1 . At both graphs the solid curve shows the situation for $\mu_1 = 0$ and $\mu_2 = 60$, the dotted ones show what happens if μ_1 changes to 25 and 40, respectively. We see that the upper part of the plot changes only a little, while for smaller values of V_g the change of μ_1 reveals an additional structure.

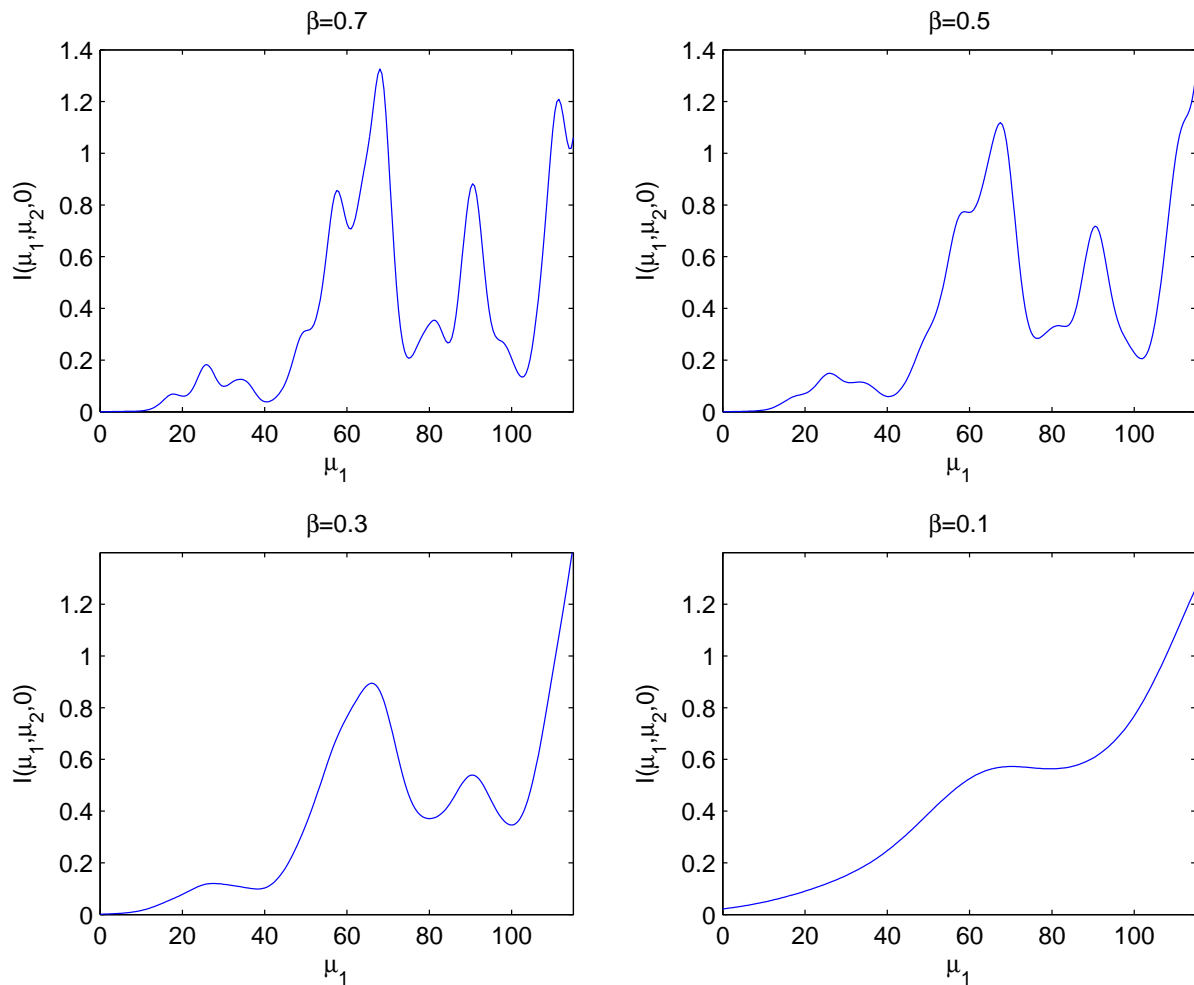


Figure 6. The current I_∞ as a function of μ_1 in the ballistic regime for $V = 2$ and a sequence of increasing temperatures corresponding to $\beta = 0.7, 0.5, 0.3, 0.1$.

Acknowledgments

The research was supported by the Czech Science Foundation within the project 14-06818S. VAZ is thankful to Valeriu Moldoveanu for instructive discussions concerning, in particular, the numeric implementation of the non-equilibrium current analysis in the case of discrete geometric scatterers. The authors also acknowledge hospitality extended to them during the respective visits: VAZ and HN to the Nuclear Physics Institute ASCR, the stay which triggered this paper, and PE to Centre de Physique Théorique, CNRS, Marseille-Luminy.

References

- [AJPP] W. Aschbacher, V. Jakšić, Y. Pautrat, C.-A. Pillet : Transport properties of quasi-free fermions, *J. Math. Phys.* **48** (2007), 032101-28.
- [AJP] S. Attal, A. Joye, C.-A. Pillet, eds.: *Open Quantum Systems, I. The Hamiltonian Approach, II. The Markovian Approach, III. Recent Developments*, Lecture Notes in Mathematics,

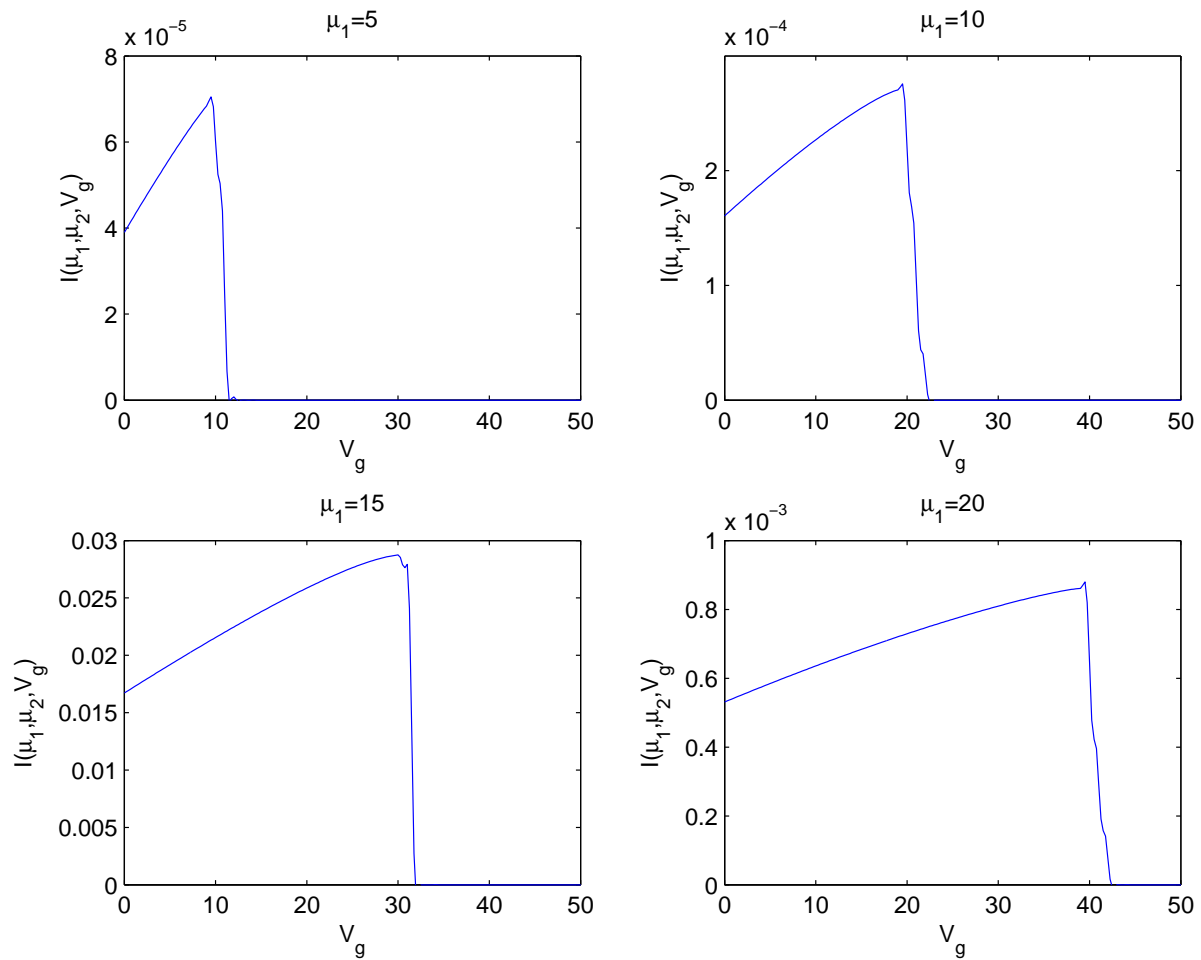


Figure 7. Variation of the current I_∞ in the non-ballistic regime on the plunger-gate voltage V_g for fixed $V = 1$ and different values of $\mu_1 = 5, 10, 15, 20$, with $\beta = 25$.

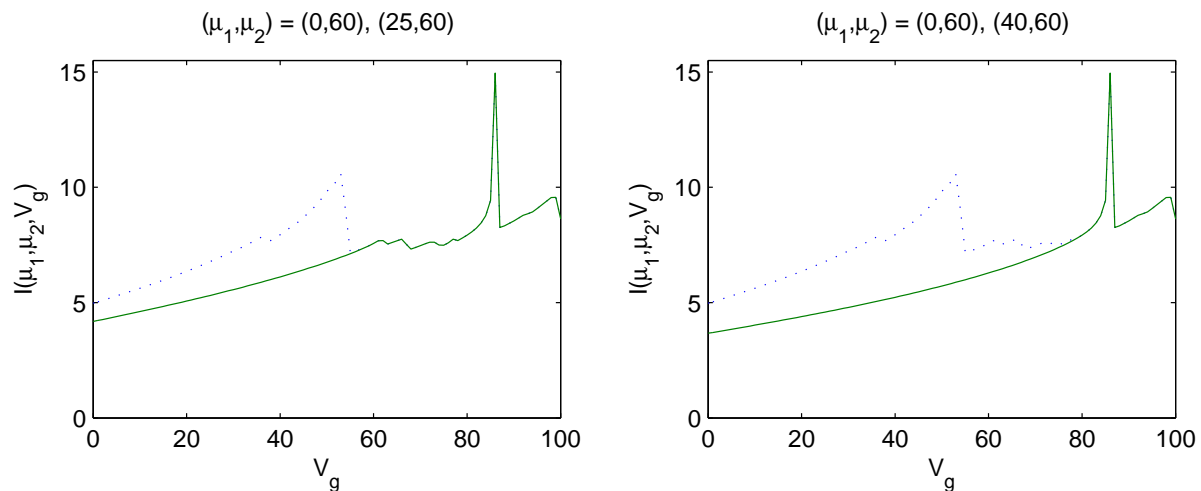


Figure 8. Change of the current due to variation of V , with $\beta = 25$. The solid curve refers to $\mu_1 = 0, \mu_2 = 60$, the dotted ones to two other values of μ_1 .

- vols. **1880-1882**, Springer-Verlag, Berlin-Heidelberg 2006.
- [BGMP02] J.Brüning, V.A. Geyler, V.A. Margulis, M.A. Pyataev: Ballistic conductance of a quantum sphere, *J. Phys. A: Math. Gen.* **35** (2002), 4239–4247.
- [CGZ10] H. Cornean, C. Giancesello, V. Zagrebnov: A partition-free approach to transient and steady-state charge currents, *J. Phys. A: Math. Theor.* **43** (2010), 474011.
- [CJM06] H. Cornean, A. Jensen, V. Moldoveanu: The Landauer-Büttiker formula and resonant quantum transport, in “Selected and Refereed Lectures from QMath9” (J.Asch and A. Joye, eds.), *Springer Lect. Notes Phys.* **690** (2006), 45–53.
- [EŠ87] P. Exner, P. Šeba: Quantum motion on a halfline connected to a plane, *J. Math. Phys.* **28** (1987), 386–381, 2254.
- [EŠ97] P. Exner, P. Šeba: Resonance statistics in a microwave cavity with a thin antenna, *Phys. Lett. A* **228** (1997), 146–150.
- [ETV01] P. Exner, M. Tater, D. Vaněk: Evanescent modes in multiple scattering factorization, *J. Math. Phys.* **42** (2001), 4050–4078.
- [Ju80] C. Jung: An exactly soluble three-body problem in one dimension, *Canadian J. Phys.* **58** (1980), 719–728.
- [Ki97] A. Kiselev: Some examples in one-dimensional “geometric” scattering on manifolds, *J. Math. Anal. Appl.* **212** (1997), 263–280.
- [KS99] V. Kostrykin, R. Schrader: Kirchhoff’s rule for quantum wires, *J. Phys. A: Math. Gen.* **32** (1999), 595–630.
- [RS78] M. Reed, B. Simon: *Methods of Modern Mathematical Physics, IV. Analysis of Operators*, Academic Press, New York 1978.